Journal of Marine Research, 55, 201–222, 1997

Subduction of water masses in an eddying ocean

by David Marshall[1]

ABSTRACT

Mesoscale eddies modify the rate at which a water mass transfers from the surface mixed layer of the ocean into the interior thermocline, in particular in regions of intense baroclinic instability such as the Antarctic Circumpolar Current, open-ocean convective chimneys, and ocean fronts. Here, the time-mean subduction of a water mass, evaluated following the meandering surface density outcrops, is found to incorporate a rectified contribution from eddies, arising from correlations between the area over which the water mass is outcropped at the sea surface and the local subduction rate. Alternatively, this eddy subduction can be interpreted in terms of an eddy-driven secondary circulation associated with baroclinic instability. The net subduction rate, incorporating both Eulerian-mean and eddy contributions, can be further related to buoyancy forcing of the surface mixed layer using a formula by Walin (1982).

Solutions from an idealized two-dimensional ocean model are presented to illustrate the eddy contribution to subduction rates in the Southern Ocean and in an open-ocean convective chimney. In the Southern Ocean, the net subduction rate is the residual of the Eulerian-mean and eddy contributions, which cancel at leading order; given plausible patterns of surface buoyancy forcing, one can obtain subduction of Antarctic Intermediate Water and Antarctic Bottom Water, with entrainment of North Atlantic Deep Water in between. In a convective chimney, in contrast, the Eulerian-mean subduction rate is vanishingly small and the subduction is contributed entirely by mesoscale eddies.

1. Introduction

The large-scale transfer—"subduction"—of fluid from the surface mixed layer into the interior thermocline determines the rate at which the surface water-mass properties are communicated into the interior of the ocean. Understanding the underlying causes of subduction, and quantifying large-scale subduction rates, is therefore one of the foremost challenges facing physical oceanographers. While much progress has been made in describing the mechanics and thermodynamics of subduction (Walin, 1982; Cushman-Roisin, 1987; Nurser and Marshall, 1991; Marshall and Nurser, 1992), the role of mesoscale eddies in the subduction mechanism has remained obscure. This is despite compelling observational and theoretical evidence that the mesoscale contribution to subduction might be considerable. For example:

- Tracer distributions in the Southern Ocean indicate the subduction of two important

1. Department of Meteorology, University of Reading, P.O. Box 243, Reading RG6 6BB, United Kingdom.

water masses—Antarctic Intermediate Water (AAIW) and Antarctic Bottom Water (AABW)—with entrainment (that is, negative subduction) of North Atlantic Deep Water (NADW) in between. These water mass distributions are completely at odds with the Eulerian-mean meridional circulation, dominated by the wind-driven Deacon Cell.

- The net vertical motion generated within an open-ocean convective chimney is vanishingly small (Send and Marshall, 1995), suggesting that the net production of deep water cannot exceed the volume of the chimney. In a prolonged convection event, however, baroclinic eddies can disperse the convective products away from their formation site (Visbeck *et al.,* 1996) leading to a significant enhancement of the overall subduction rate.
- Observations from the FASINEX program (Pollard and Regier, 1992) reveal frontal instabilities including a transient transfer of fluid between the mixed layer and thermocline. Scaling arguments (Follows and Marshall, 1994) and numerical modeling (Spall, 1995) suggest that this transient, frontal subduction might be comparable with large-scale climatological subduction rates.

The aims of this paper are:

(i) to develop a simple framework for interpreting and diagnosing the mesoscale contribution to the subduction of a water mass;

(ii) to establish the relation between the net subduction rate and surface buoyancy forcing;

(iii) to estimate the contribution of eddies to subduction rates in the Southern Ocean and convective chimneys.

In Section 2, the time-mean subduction of a water mass is shown to incorporate an eddy contribution, associated with correlations between the area over which the water mass is outcropped, and the local subduction rate. In Section 3, this eddy contribution is reinterpreted in terms of an eddy-driven "bolus" circulation across the base of the mixed layer. In Section 4, the net subduction rate, incorporating both mean and eddy components, is further related to the buoyancy forcing of the surface mixed layer. In Section 5, the application of these ideas to the Southern Ocean and an open-ocean convective chimney is illustrated using a simple two-dimensional ocean model. Finally, in Section 6, wider implications of these results, both for the ocean and for numerical ocean models, are discussed further.

2. Time-mean subduction of a water mass

Subduction is the transfer of fluid from the surface mixed layer of the ocean into the interior thermocline. This transfer is quantified by the "subduction rate," S, which

measures the volume flux, per unit surface area, across the sloping base of the mixed layer. Here we shall consider only a two-dimensional ocean in which, following Cushman-Roisin (1987),

$$S = -\left\{\frac{\partial h}{\partial t} + v_b \frac{\partial h}{\partial y} + w_b\right\}, \tag{1}$$

where (v_b, w_b) is the fluid velocity at the base of the mixed layer, $z = -h$. Subduction is achieved through either shallowing of the mixed layer, lateral transfer of fluid across the sloping mixed-layer base, or through vertical motion.

Over much of the ocean, such as the subtropical gyres of the North Atlantic and North Pacific, the large-scale subduction of water masses is dominated by Eulerian-mean advection, and one can estimate climatological subduction rates by substituting Eulerian-mean velocities into (1) directly (Marshall *et al.*, 1993; Huang and Qiu, 1994).

However, in regions of intense baroclinic instability, such as those highlighted in Section 1, the contribution of an ensemble of eddies to the large-scale, time-mean subduction rate is potentially of the same order and cannot be neglected. But how can one quantify the net contribution of eddies to the subduction of a water mass? A simple Eulerian time-average of Eq. (1) is not appropriate since the surface area over which the water mass is outcropped is itself evolving. Instead one must evaluate the time-mean subduction rate: (i) in a Lagrangian frame of reference which follows the meandering surface density outcrops, and (ii) taking account of the area over which the water mass is outcropped, as illustrated schematically in Figure 1.

The net subduction of the water mass, defined to lie within a density range $\rho_1 \leq \rho \leq \rho_2$, is therefore given by the local subduction rate, $S(t)$, multiplied by spacing, $\Delta y(t)$, between the two bounding outcrops, ρ_1 and ρ_2. Separating the fluid variables into "mean" and "eddy" components, $v = \bar{v} + v'$, $h = \bar{h} + \Delta h'$, etc, where the "mean" represents a low-pass time-filtering operation over several baroclinic eddy life-cycles, one finds

$$\overline{S(t)\Delta y(t)} = -\left\{\frac{\partial \bar{h}}{\partial t}\overline{\Delta y} + \bar{v}_b \frac{\partial \bar{h}}{\partial y}\overline{\Delta y} + \overline{w}_b \overline{\Delta y}\right\} - \overline{\left\{\frac{\partial h}{\partial t} + v_b \frac{\partial h}{\partial y} + w_b\right\}' \Delta y'} - \overline{v_b' \frac{\partial h'}{\partial y}}\,\overline{\Delta y}.$$

Finally, dividing by the mean outcrop spacing gives an expression for the "water-mass subduction rate" per unit surface area,

$$\overline{S}^{WM} \equiv \frac{\overline{S\Delta y}}{\overline{\Delta y}} = S_{\text{Eulerian}} + S_{\text{eddy}}, \tag{2}$$

where

$$S_{\text{Eulerian}} = -\left\{\frac{\partial \bar{h}}{\partial t} + \bar{v}_b \frac{\partial \bar{h}}{\partial y} + \overline{w}_b\right\} \tag{3}$$

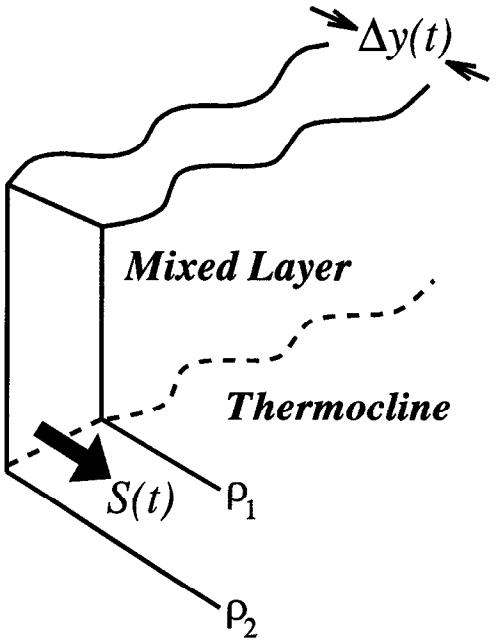

Figure 1. The time-mean subduction of a water mass, defined to lie within a density range $\rho_1 \leq \rho \leq \rho_2$, is given by the product of the instantaneous subduction rate, $S(t)$, and the area over which the water mass is outcropped at the sea surface, $\Delta y(t)$. The solid lines represent isopycnals and the dashed line is the base of the mixed layer.

is the subduction rate evaluated using Eulerian-mean velocities, and

$$S_{\text{eddy}} = -\frac{1}{\overline{\Delta y}}\overline{\left\{\frac{\partial h}{\partial t} + v_b\frac{\partial h}{\partial y} + w_b\right\}'\Delta y'} - \overline{v_b'\frac{\partial h'}{\partial y}} \tag{4}$$

is the additional subduction resulting from mesoscale eddies. The superscript on $\overline{S}^{WM}$ indicates that the averaging is performed in a Lagrangian frame which both follows the meandering water-mass outcrops, and is also weighted by the surface outcrop area. Note that a simple Eulerian average of (1) yields an incorrect result involving only the final term in (4).

In an eddying ocean, the rate at which a water mass is transferred from the surface mixed layer into the ocean interior need not coincide with the direction of the Eulerian-mean velocities and, as we shall see in Section 5, can indeed reverse when the contribution of eddies is included.

3. Relation of eddy subduction to the bolus velocity

The water-mass subduction rate, $\overline{S}^{WM}$, makes explicit the importance of eddies in the overall transfer between the mixed layer and thermocline. However, Eq. (4) is not in an

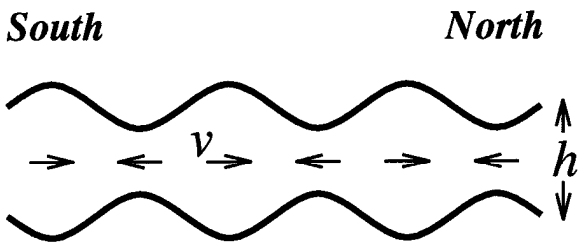

Figure 2. A schematic diagram illustrating the concept of the "bolus" transport. The solid lines represent two isopycnals defining the upper and lower bounds on a particular water mass; the fluid velocity is v and the thickness of the water-mass layer is Δz. The net transport is $T = v\Delta z$, and can remain finite even when the Eulerian-mean fluid velocity $\bar{v}$ is zero, as shown in the figure. This is because a greater volume of fluid is moving north (when Δz is large) than is returning south (when Δz is small).

ideal form with which to diagnose eddy subduction rates from observations, or to parameterize eddy subduction in a numerical ocean model. In this section, the eddy subduction rate is rewritten in terms of an eddy-induced "bolus" velocity. First the concept, definition and properties of the bolus velocity are reviewed, and then the net subduction rate is reinterpreted using the bolus velocity.

a. Definition and properties of the bolus velocity. Following Gent *et al.* (1995), consider a water mass, defined to lie within a prescribed density range, $\rho_1 \leq \rho \leq \rho_2$, and with a vertical layer thickness Δz. The water-mass transport, T, is the product of the velocity and layer thickness,

$$T = v\Delta z,$$

and the time-mean water-mass transport is

$$\overline{T} = \bar{v}\overline{\Delta z} + \overline{v'\Delta z'}.$$

Thus, there can be a net transport even when the Eulerian-mean velocity, $\bar{v}$, is vanishingly small. The physical origin of the additional term, $\overline{v'\Delta z'}$, the "bolus" transport (Rhines, 1982; McDougall, 1991), is illustrated in Figure 2. The Eulerian-mean velocity is zero, but the correlation between the fluid velocity and the perturbation layer thickness means that a greater volume of fluid is transported north when $v > 0$, than is transported south when $v < 0$. If one were to inject a passive tracer into the water-mass layer, one would observe a biased transport of tracer to the north, a result that has recently been confirmed in eddy-resolving numerical experiments by Lee *et al.* (1997).

Thus geostrophic eddies not only diffuse tracers along isopycnals, but also provide an additional *advection* by the "bolus velocity," the *isopycnal* component of which is defined:

$$v^*_\rho = \frac{\overline{v'\Delta z'}}{\overline{\Delta z}}. \tag{5}$$

The horizontal and vertical components, v^* and w^*, can be inferred using Eq. (5) along with the continuity condition,

$$\frac{\partial v^*}{\partial y} + \frac{\partial w^*}{\partial z} = 0, \tag{6}$$

and boundary conditions of zero normal component at solid boundaries and at the sea surface.

The sum of the Eulerian-mean and bolus velocities is the "transport velocity,"[2] and it is this latter quantity which controls the advective spreading of tracers. The transport velocity satisfies a continuity equation,

$$\frac{\partial}{\partial y}(\bar{v} + v^*) + \frac{\partial}{\partial z}(\bar{w} + w^*) = 0, \tag{7}$$

and, within the interior of the ocean, an important adiabatic relation,

$$\frac{\partial \bar{\rho}}{\partial t} + (\bar{v} + v^*)\frac{\partial \bar{\rho}}{\partial y} + (\bar{w} + w^*)\frac{\partial \bar{\rho}}{\partial z} = F_\rho, \tag{8}$$

where $\bar{\rho}$ is the mean density[3] and F_ρ is the explicit buoyancy forcing (taken to include any diapycnal mixing, for example, associated with the breaking of internal waves). Thus in the absence of explicit buoyancy forcing, the transport velocities are unable to transfer fluid across mean isopycnals—the eddies are "adiabatic" in the sense that they redistribute water along density surfaces, but do not modify the density of any individual fluid parcel. This is a good approximation within the interior of the ocean; within the surface mixed layer, however, this adiabatic approximation breaks down and, following Treguier *et al.* (1997), and diapycnal mixing by geostrophic eddies must be included in the definition of F_ρ.

b. Expression for eddy subduction using the bolus velocity. The transport velocities provide a succinct and elegant framework for describing water-mass transport in an eddying ocean. The following physically-motivated derivation shows how subduction rates in an eddying ocean can also be described in terms of these same transport velocities.

First, consider the area, A, contained between the base of a mixed layer, the two bounding isopycnals ρ_1 and ρ_2, and a fixed Eulerian location $y = y_0$, as sketched in Figure 3a. The surface outcrops are separated by a distance $\Delta y(t) = y(\rho_2) - y(\rho_1)$, and the vertical spacing between the isopycnals at y_0 is $\Delta z(t)$. Noting that the isopycnals are

2. The transport velocity is closely related, though not identical, to the "residual-mean velocity" of Andrews and McIntyre (1976) and the "Lagrangian-mean velocity" of Andrews and McIntyre (1978). A helpful discussion of these various definitions, and the situations under which they are equivalent, is given by Andrews *et al.* (1987).

3. McDougall and McIntosh (1996) have shown that $\bar{\rho}$ in Eq. (8) formally represents the *density of the isopycnal whose mean depth is z*, rather than a simple Eulerian average of ρ at a fixed depth. This subtle distinction will prove important in deriving an exact correspondence between the eddy subduction and bolus velocity in Section 3b.

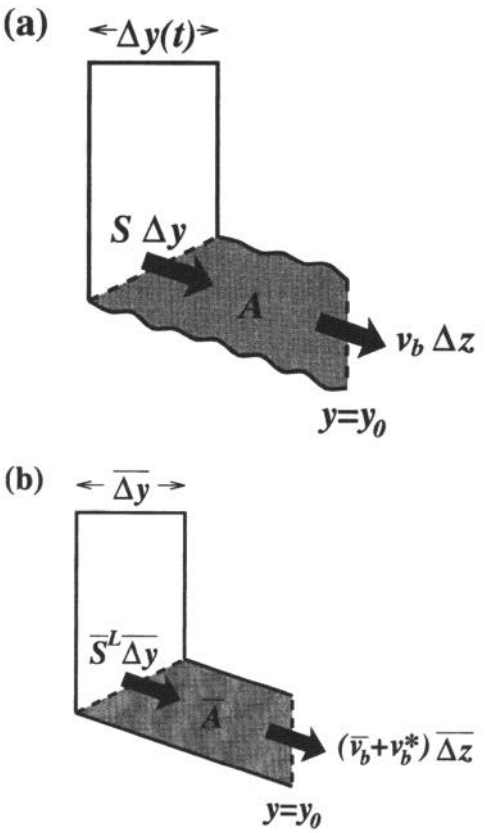

Figure 3. (a) The shaded area, A, contained between the two density surfaces, ρ_1 and ρ_2, can be modified either through a subduction of fluid from the surface mixed layer or through a lateral water-mass transport at $y = y_0$. Here Δz is the vertical separation of the isopycnals within the thermocline. (b) Likewise the area, $\overline{A}$, contained between the same density surfaces plotted at their time-mean depths, is modified either through the subduction, $\overline{S}^{WM}$, defined using transport velocities, or through a lateral transport velocity at $y = y_0$.

material surfaces since the thermocline is adiabatic, the area A can change only through subduction from the surface mixed layer, or a lateral transport across $y = y_0$, that is

$$\frac{\partial A}{\partial t} = S\Delta y - v_b \Delta z.$$

Averaging over several eddy life-cycles gives

$$\frac{\partial \overline{A}}{\partial t} = \overline{S\Delta y} - (\overline{v_b} + v_b^*)\overline{\Delta z}. \tag{9}$$

Now, consider an analogous problem for the area, $\overline{A}$, contained between the time-mean

isopycnals, $\overline{\rho}_1$ and $\overline{\rho}_2$, the mixed layer, and y_0, as sketched in Figure 3b.[4] The mean isopycnals are material surfaces for the transport velocities, and thus the area, $\overline{A}$, can change only through a transport velocity directed across the sloping mixed-layer base, or a lateral transport velocity across $y = y_0$. Analogous to (9), we find

$$\frac{\partial \overline{A}}{\partial t} = -\left\{\frac{\partial \overline{h}}{\partial t} + (\overline{v_b} + v_b^*)\frac{\partial \overline{h}}{\partial y} + (\overline{w_b} + w_b^*)\right\}\overline{\Delta y} - (\overline{v_b} + v_b^*)\overline{\Delta z}. \tag{10}$$

Finally, equating (9) and (10), the water-mass subduction rate defined in (2) is simply

$$\overline{S}^{WM} = -\left\{\frac{\partial \overline{h}}{\partial t} + (\overline{v_b} + v_b^*)\frac{\partial \overline{h}}{\partial y} + (\overline{w_b} + w_b^*)\right\}. \tag{11}$$

The water-mass subduction rate is therefore equivalent to the subduction rate written in terms of transport velocities. Physically, it is the transport velocities that advect temperature, salinity, and other tracers across the base of the mixed layer, and therefore lead to subduction of water-masses.

In particular, the additional subduction provided by mesoscale eddies is

$$S_{\text{eddy}} = -\left\{v_b^*\frac{\partial \overline{h}}{\partial y} + w_b^*\right\}, \tag{12}$$

and is readily interpreted as the rectified water-mass transport across the sloping base of the mixed layer by the eddy-induced bolus velocity. The bolus velocity is generally largest in regions of intense baroclinic instability (Gent *et al.*, 1995) and thus it is in such regions that one expects eddies to contribute most significantly to subduction rates.

4. Relation of subduction to surface forcing

The net subduction rate, incorporating both Eulerian-mean and eddy contributions, is now related to buoyancy forcing of the surface mixed layer using the approach of Walin (1982). The need to satisfy such a relation has been noted independently by Tandon and Garrett (1996).

Following Walin (1982), consider a column of mixed-layer fluid, exposed to a surface buoyancy flux, $\mathscr{B}_{\text{in}}$, and smoothly overlying an adiabatic thermocline. The column is bounded by two time-mean isopycnals, $\overline{\rho}_1$ and $\overline{\rho}_2$; the lateral spacing between the outcropped density surfaces is $\overline{\Delta y}$ and within the thermocline the vertical spacing between the same isopycnals is $\overline{\Delta z}$. The ocean is assumed in a statistically-steady state.

a. Volume budget. First consider a volume budget for the fluid column—Figure 4a. Integrating the continuity Eq. (7) over the mixed layer column and noting that the transport

4. Here the volume of fluid contained between the time-mean isopycnals, $\overline{\rho}_1$ and $\overline{\rho}_2$, is assumed equivalent to the time-mean volume of fluid contained between the instantaneous isopycnals, ρ_1 and ρ_2. This is exact provided that one properly defines "mean isopycnals" according to the recipe outlined in footnote 3.

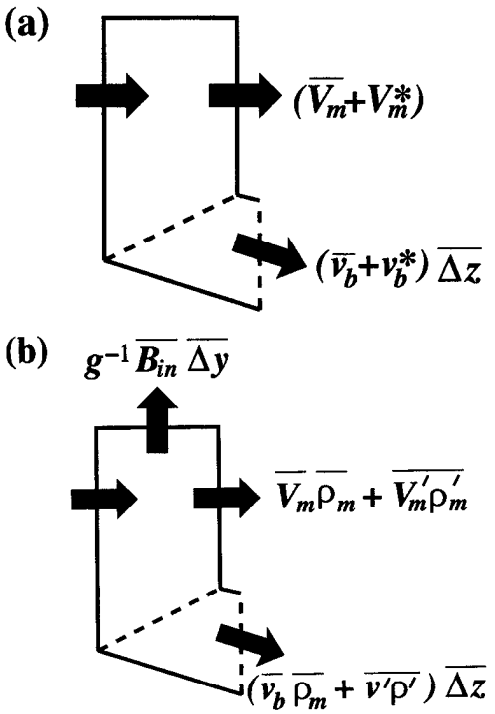

Figure 4. (a) A convergence of the transport velocities within the surface mixed layer, $\Delta(\overline{V}_m + V_m^*)$, must be balanced by a transport velocity, $(\overline{v_b} + v_b^*)\overline{\Delta z}$, at the base of the mixed layer. The solid lines are time-mean density surfaces. (b) A buoyancy budget for the same mixed-layer fluid column: the buoyancy can be modified either through a surface buoyancy flux, a convergence of lateral buoyancy fluxes within the mixed layer, or a transport of buoyancy into the thermocline.

velocities do not cross isopycnals within the thermocline, we find

$$\frac{\partial}{\partial y}\int_{-\bar{h}}^{0}(\overline{v_m} + v_m^*)dz\overline{\Delta y} + (\overline{v_b} + v_b^*)\overline{\Delta z} = 0. \tag{13}$$

Here v_m and v_m^* are the horizontal components of the Eulerian-mean, and eddy-induced velocities within the mixed layer, and v_b and v_b^* are the same velocity components at the base of the mixed layer.

b. Buoyancy budget. Likewise consider the time-mean buoyancy budget for the same fluid column—Figure 4b. The buoyancy can be modified either by a surface buoyancy flux, Eulerian-mean advection, or eddy buoyancy fluxes,

$$\frac{\partial}{\partial y}\int_{-\bar{h}}^{0} g[\overline{v_m\rho_m} + \overline{v_m'\rho_m'}]\,dz\overline{\Delta y} + g[\overline{v_b\rho_m} + \overline{v'\rho'}|_b]\overline{\Delta z} + \overline{\mathscr{B}_{\text{in}}\Delta y} = 0. \tag{14}$$

Here, $\overline{v'\rho'}|_b$ is the lateral eddy heat flux at the base of the mixed layer and is purely advective,

$$\overline{v'\rho'}|_b = v_b^*\overline{\rho_m},$$

since the diffusive flux of density along an isopycnal surface is zero by definition. However the eddy buoyancy flux within the mixed layer, $\overline{v_m'\rho_m'}$, includes both advective and diffusive components due to diabatic mixing along the sea surface,

$$\overline{v_m'\rho_m'} = v_m^*\overline{\rho_m} - \gamma\frac{\partial\rho_m}{\partial y},$$

where γ is the diapycnal mixing coefficient within the mixed layer (Treguier *et al.*, 1997; also see Section 3a). Combining (13) and (14) gives a mixed-layer buoyancy equation,

$$\int_{-\bar{h}}^{0}(\overline{v_m} + v_m^*)\,dz\,\frac{\partial\overline{\rho_m}}{\partial y} = \frac{(\overline{\mathscr{B}_{\text{in}}} + \mathscr{B}_{\text{eddy}})}{g}, \tag{15}$$

where

$$\mathscr{B}_{\text{eddy}} = g\frac{\partial}{\partial y}\left\{\gamma h\frac{\partial\overline{\rho_m}}{\partial y}\right\}$$

is the buoyancy forcing associated with the diabatic mixing of adjacent mixed-layer fluid columns.[5]

c. Subduction rate. Eliminating $(\overline{v_m} + v_m^*)$ between (13) and (15) gives

$$(\overline{v_b} + v_b^*)\overline{\Delta z} = \frac{\partial}{\partial y}\left\{\frac{\overline{\mathscr{B}_{\text{in}}} + \mathscr{B}_{\text{eddy}}}{g\partial\overline{\rho_m}/\partial y}\right\}\overline{\Delta y}.$$

However, since the motion is statistically steady, $(\overline{v_b} + v_b^*)\overline{\Delta z}$ is equivalent to the net subduction rate, $\overline{S^{WM}\Delta y}$, by Eq. (10). Thus,

$$\overline{S}^{WM} = \frac{\partial}{\partial y}\left\{\frac{\overline{\mathscr{B}_{\text{in}}} + \mathscr{B}_{\text{eddy}}}{g\partial\overline{\rho_m}/\partial y}\right\}. \tag{16}$$

The rate at which a water mass is subducted from the surface mixed layer into the thermocline beneath is related simply to the air/sea buoyancy flux and the buoyancy forcing associated with diapycnal mixing within the surface mixed layer (Walin, 1982). This result can be extended to a time-dependent ocean, provided that one integrates over a self-repeating cycle such as a closed seasonal cycle. Note that the eddy heat flux entrained through the base of the mixed layer makes no contribution to the right-hand side of Eq. (16)—physically, the eddies transport fluid adiabatically along density surfaces, but lead to no transformation of water masses between adjacent density classes.

5. Alternatively, one can obtain (15) by setting $\partial/\partial t = 0$ in Eq. (8) and integrating over the depth of the mixed layer.

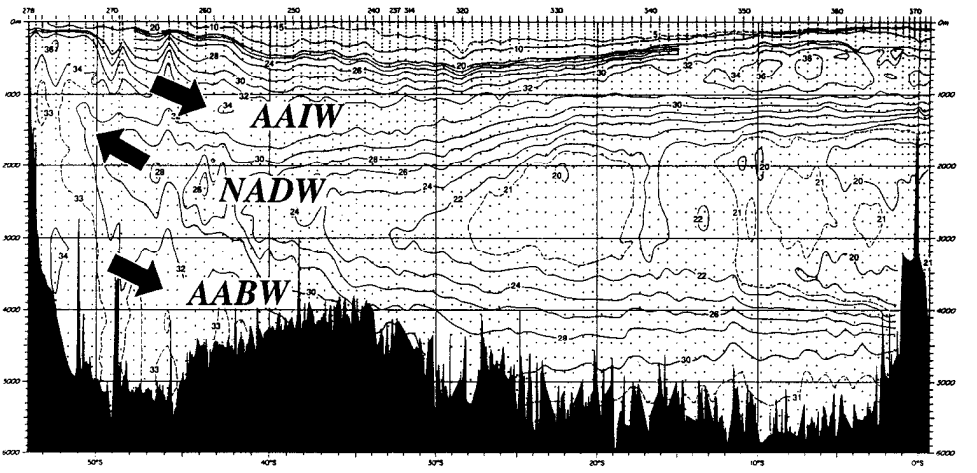

Figure 5. A meridional section of nitrate in the western North Atlantic (adapted from Tsuchiya *et al.*, 1994). The high values are indicative of the two Antarctic Water Masses—AAIW and AABW—whereas the lower values in between indicate water of North Atlantic origin—NADW.

Eq. (16) is a special case of an extremely general relation between the transport velocities and buoyancy forcing in a two-dimensional, statistically-steady ocean. More generally, consider the buoyancy equation, (8): the transport velocity vectors, $(\overline{\mathbf{v}}+\mathbf{v}^*)$, are only able to pass across density contours in the presence of finite buoyancy forcing, F_ρ; given both F_ρ and the distribution of density surfaces, one can uniquely determine the diapycnal component of the transport velocity; the isopycnal component of the transport velocity then follows from continuity. Thus, while more detailed buoyancy terms, such as entrainment fluxes, have been excluded here, they could in principle be included as additional terms on the right-hand side of Eq. (16), even if practical use of the relation would then be restricted to numerical models in which such terms could be evaluated explicitly (Garrett *et al.*, 1995; Nurser *et al.*, 1997). This fundamental relation between the transport velocities and buoyancy forcing in the ocean is directly analogous to a relation between the transport circulation and diabatic forcing of the stratosphere (Tung, 1987).

5. Examples

Solutions from an idealized two-dimensional ocean model are now considered to illustrate how eddies can modify the water-mass subduction rate, and the relation of the subduction to surface buoyancy forcing. Two oceanographic examples, the Southern Ocean and an open-ocean convective chimney, are considered.

a. Southern Ocean. Meridional tracer distributions in the Southern Ocean (Fig. 5) indicate the subduction of two Antarctic water masses—Intermediate Water (AAIW) and Bottom Water (AABW), with entrainment of North Atlantic Deep Water (NADW) in between.

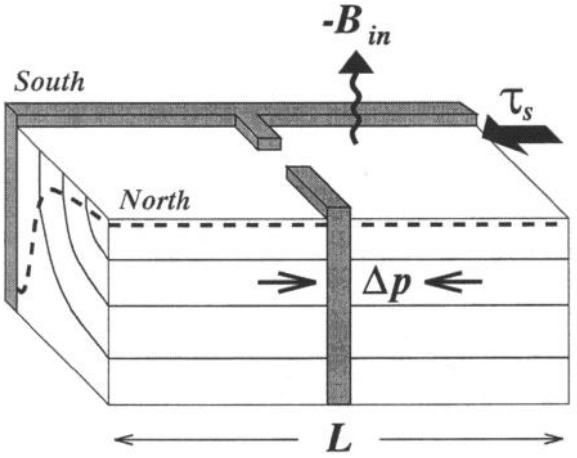

Figure 6. The two-dimensional Southern Ocean model consists of a zonal channel exposed at its surface to a wind-stress, τ_s, and an air/sea buoyancy flux, $\mathscr{B}_{in}$. Dissipation is through a prescribed zonal pressure gradient, Δp, across a partial barrier representing the Drake Passage. The channel is bounded to the south by Antarctica, but is open at its northern edge. The solid lines represent isopycnals and the dotted line represents the base of the mixed layer.

These tracer-inferred subduction rates are at odds with the Eulerian-mean circulation, dominated by the Deacon Cell which upwells over the circumpolar ocean and downwells to the north. Danabasoglu *et al.* (1994), employing the Gent and McWilliams (1990) parameterization of $\mathbf{v}^*$, have evaluated the bolus velocities in a course-resolution ocean general circulation model. They find that the Deacon Cell is greatly reduced when one evaluates the meridional circulation using both $\overline{\mathbf{v}}$ and $\mathbf{v}^*$, suggesting that the Deacon Cell is largely an artifact of an Eulerian averaging procedure, analogous to the Ferrell cell in the atmosphere (Plumb and Mahlman, 1987). The near cancellation of the Deacon Cell is not, however, a general result obtained in all ocean models. For example, the eddy-resolving FRAM integration retains a finite interior transport circulation directed predominantly along density surfaces (Döös and Webb, 1994; McIntosh and McDougall, 1996); and more recent experiments by Danabasoglu and McWilliams (1995), in which the Gent and McWilliams parameterization is turned off within the upper boundary layer, retain a sizable surface Deacon cell. The aim of the following calculations is to illustrate and explain these results using the subduction ideas developed in Sections 2–4.

The model, sketched schematically in Figure 6, consists of a zonally-symmetric channel, within which a vertically-homogeneous surface mixed layer of prescribed density and depth overlies an adiabatic thermocline. The mixed-layer depth varies linearly with latitude except for a sharp increase adjacent to Antarctica. The meridional extent is 2000 km and the ocean depth is 4 km. The model is forced by a prescribed surface wind stress, τ_s, and is dissipated by a prescribed zonal pressure gradient, Δp, across a partial barrier representing the Drake Passage. An air/sea buoyancy flux, $\mathscr{B}_{in}$ is also prescribed at the sea surface; the

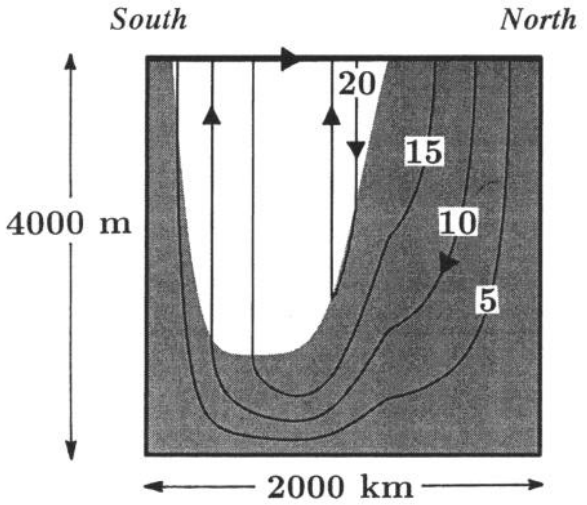

Figure 7. The stream function for the Eulerian-mean meridional circulation, evaluated using the Eulerian-mean velocity, $\bar{v}$. This is dominated by the wind-driven Deacon Cell, with upwelling over the circumpolar belt. Shading indicates the extent of the topographic barrier where the zonal pressure gradient is finite; in contrast the zonal pressure gradient is zero within the unshaded latitude and depth range of the Drake Passage.

eddy buoyancy term, $\mathcal{B}_{\text{eddy}}$ is negligible due to the large-meridional scale and a uniform mixed-layer density gradient. The eddy-induced bolus velocity is parameterized following Gent and McWilliams (1990). Full details of the model are given in the Appendix.

The Eulerian-mean meridional circulation (Fig. 7) consists of a classical Deacon Cell with slightly in excess of 20 Sv sinking to the north and an equal volume of fluid upwelling to the south. Shading in Figure 7 indicates the latitude and depth range obstructed by topography where the zonal pressure gradient is finite. The Eulerian-mean meridional circulation is independent of both the surface buoyancy forcing and the stratification of the thermocline in this idealized model in which mechanical forcing is prescribed *a priori.*

The meridional transport circulation, in contrast, is determined entirely by the surface buoyancy forcing. Two solutions are presented in which different surface buoyancy fluxes are prescribed:

- The first solution (Fig. 8a) is with zero surface buoyancy flux. The bolus velocities exactly cancel the Eulerian-mean velocities such that the total transport circulation vanishes, consistent with the generalized subduction formula, Eq. (16). Note that the slope of the isopycnals is sensitive to the arbitrary choice of transfer coefficient in the Gent and McWilliams parameterization (here $\kappa = 500\ \text{m}^2\ \text{s}^{-1}$); however the strength of the eddy-induced bolus circulation, and hence the cancellation of the Deacon Cell, is not.

- The second solution (Fig. 8b) incorporates two regions of surface buoyancy loss, the

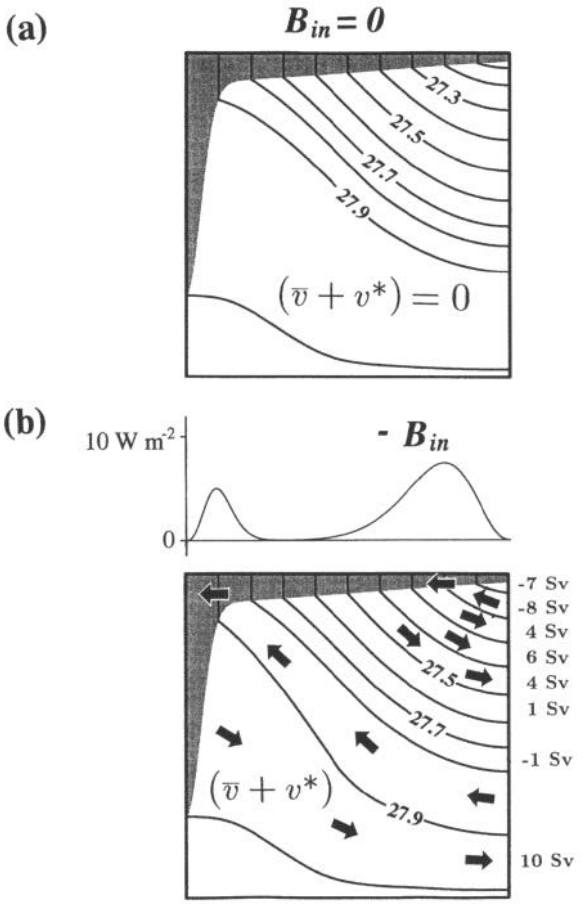

Figure 8. Meridional section and transport velocities for two distributions of surface buoyancy forcing. The solid lines are isopycnals (kg m^{-3}) and the mixed layer is shaded. (a) Solution in which $\mathscr{B}_{in} = 0$: the eddy-induced bolus velocity exactly cancels the Eulerian-mean velocity and there is no net subduction. (b) Solution with two regions of surface buoyancy loss: there is subduction of both AAIW (15 Sv) and AABW (10 Sv) with entrainment of NADW (10 Sv) in between. Note the modification to the isopycnal slopes in order to support the additional bolus transports. Within the thermocline, the transport velocities are directed entirely along isopycnals. The buoyancy flux is shown as an equivalent heat loss (W m^{-2})—multiply by 5×10^{-7} to convert back to a buoyancy flux (kg m^{-1} s^{-3}).

first over the circumpolar belt and the second adjacent to Antarctica. The Eulerian-mean, and bolus velocities no longer exactly cancel, but leave two residual bands of subduction—AAIW and AABW—with entrainment of NADW in between. Within the thermocline, the total transport circulation is adiabatic and directed along density surfaces. Note the subtle adjustments to the isopycnals to accommodate the additional bolus velocities. Thus, if one were to inject a passive tracer into the surface

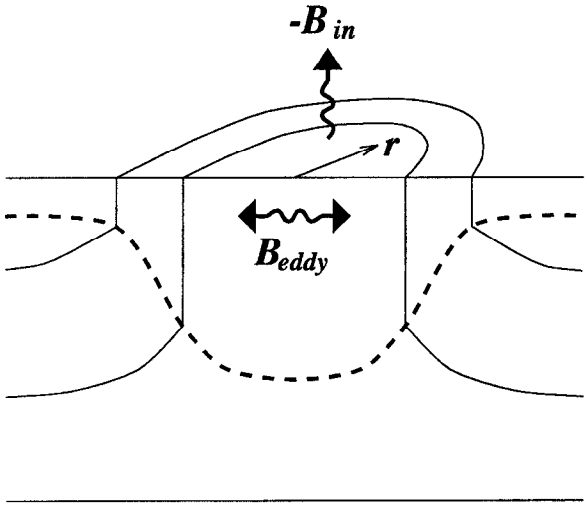

Figure 9. The cylindrically-symmetric chimney is forced by a surface buoyancy flux, $\mathscr{B}_{\text{in}}$, and a lateral buoyancy transfer within the mixed layer, $\mathscr{B}_{\text{eddy}}$.

mixed-layer, two "tongues" of tracer would subduct into the thermocline at the depths of AAIW and AABW, as observed in climatological data (Fig. 5).

The above model succeeds in highlighting the distinct roles of mechanical and buoyancy forcing in driving the Eulerian-mean and transport meridional circulations respectively. Nevertheless, the details of the partitioning of the transport circulation between transient eddies, and basin-scale standing eddies (discussed by Döös and Webb, 1994), cannot be resolved by a two-dimensional model and will require further study. A related issue concerns the distributions of air/sea buoyancy fluxes, which are simply prescribed here, but in general cannot be considered independent of the ocean circulation. The underlying causes of these fluxes, and their spatial variability, is likely to prove crucial in understanding the subduction of water masses in the Southern Ocean.

b. Open-ocean convective chimney. Open-ocean deep convection occurs in a few isolated regions such as the Mediterranean, the Greenland Sea Gyre, the Labrador Sea and the subpolar gyre. The focus here is on the prolonged "statistically-steady" convection articulated by Visbeck *et al.* (1996), in which localized buoyancy loss is compensated by a lateral influx of buoyancy by transient geostrophic eddies.

A cylindrically-symmetric domain of radius 200 km is considered, within which a vertically-homogeneous mixed-layer overlies an adiabatic thermocline, as sketched schematically in Figure 9. No mechanical forcing is applied; the model is forced only by a surface buoyancy flux, $\mathscr{B}_{\text{in}}$, and the lateral redistribution of buoyancy within the mixed layer, $\mathscr{B}_{\text{eddy}}$. The latter is parameterized as a simple down-gradient diffusion of mixed-

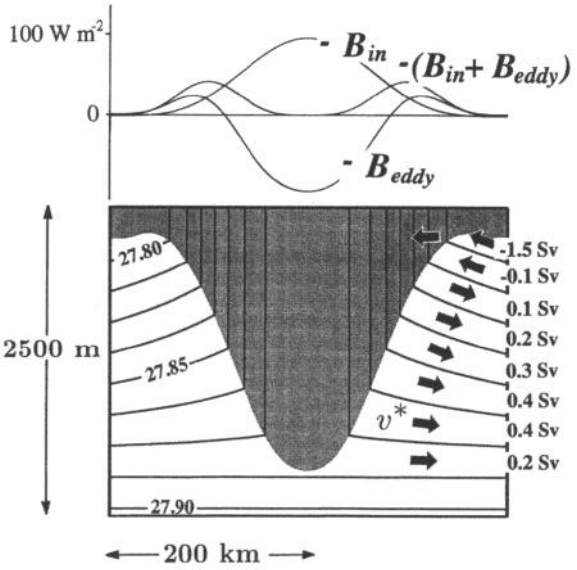

Figure 10. A solution for a convective chimney. The subduction rate is determined by the net buoyancy forcing, $\mathscr{B}_{in} + \mathscr{B}_{eddy}$, and indicates entrainment of warm, buoyant fluid over the upper kilometer, with subduction of cold, dense fluid at greater depths—the net subduction of deep water is 1.6 Sv. Solid lines are isopycnals (kg m^{-3}).

layer density. Beneath the mixed layer, the bolus velocities are again parameterized according to Gent and McWilliams (1990). Further details are given in the Appendix.

In contrast to the Southern Ocean, the Eulerian-mean circulation is identically zero—physically, the net vertical and radial motion in a convective chimney is vanishingly small due to vorticity constraints which preclude any significant stretching of vortex tubes (Send and Marshall, 1995). Thus the Eulerian-mean velocities provide zero subduction.

The subduction is therefore contributed entirely by mesoscale eddies through the eddy-induced bolus velocity. A typicaly solution is presented in Figure 10. The surface buoyancy flux is zero at the rim of the domain, increasing to -5×10^{-5} kg m^{-1} s^{-3} at its center, equivalent to a heat loss of $\sim$100 W m^{-2}. The eddy buoyancy forcing, $\mathscr{B}_{eddy}$ is equal and opposite to $\mathscr{B}_{in}$ at the center of the chimney, a necessary condition to avoid infinite subduction at $r = 0$ by Eq. (16). The buoyancy forcing results in a deep mixed layer within the chimney, and the upward doming of isopycnals toward its center. The eddy subduction is determined by the combined buoyancy forcing, $(\mathscr{B}_{in} + \mathscr{B}_{eddy})$. In the present example (Fig. 10), 1.6 Sv of Deep Water is formed within the chimney and is subducted over a range of density surfaces as indicated. Note that this net subduction rate is sensitive to the arbitrary eddy transfer coefficients, which influence the magnitude of $\mathscr{B}_{eddy}$.

The excess storage of deep water within the chimney is approximately 1.5×10^{13} m^3. Mesoscale eddies would process a similar volume in four months, suggesting that eddies

might significantly enhance the overall water-mass formation rate within such a convective chimney.

6. Discussion

Subduction rates estimated using Eulerian-mean velocities alone are inconsistent with water-mass distributions in the Southern Ocean, and also provide an incomplete picture of subduction in convective chimneys and ocean fronts. Here, a theoretical framework has been presented for diagnosing and interpreting the contribution of mesoscale eddies to the subduction of a water-mass. In particular:

- The time-mean subduction of a water mass involves an eddy correlation between the area over which the water mass is outcropped at the sea surface and the local subduction rate. In regions of intense eddy activity, the dominant direction of water-mass transfer between the mixed layer and thermocline need not coincide with the direction of the Eulerian-mean circulation.
- The additional eddy-induced subduction can be interpreted as the rectified transfer of a water mass from the mixed layer into the thermocline by an eddy-induced "bolus" velocity. The bolus velocity, and hence the eddy subduction, is largest in regions of intense baroclinic instability.
- The net subduction rate, that is including the effects of both the Eulerian-mean circulation and mesoscale eddies, is related to the buoyancy forcing of the surface mixed layer (Walin, 1982). This relation is independent of the partitioning of the subduction between Eulerian-mean and eddy contributions.

Solutions from a two-dimensional ocean model have been presented to illustrate the application of these ideas to the Southern Ocean and to a convective chimney. In the Southern Ocean, the net subduction rate is determined by the residual of the Eulerian-mean and eddy components, which cancel at leading order—given suitable distributions of surface buoyancy forcing, one can obtain a circulation scheme which includes subduction of AAIW and AABW, with entrainment of NADW in between.

In the convective chimney, the subduction is contributed entirely by the mesoscale eddies, and can lead to a significant enhancement of the overall formation rate of deep water within such a chimney. These results have some important implications for the ocean and for numerical ocean models which are now briefly mentioned.

a. Water-mass formation inferred from climatological fluxes. On the large-scale, the subduction rate for a water mass is independent of the partitioning of the subduction between mean and eddy components. This suggests that water-mass formation rates inferred from climatological air/sea buoyancy fluxes (for example, Speer and Tziperman, 1992) already implicitly account for mesoscale eddies.

b. Water-mass formation in numerical models. A corollary of the relation between subduction and buoyancy forcing, Eq. (16), is that for an ocean model to produce and subduct water masses at appropriate rates, it is imperative that the model is forced with appropriate surface buoyancy fluxes. This is disturbing because the surface fluxes, and other buoyancy terms such as entrainment fluxes, are extremely poorly determined. Of course, in reality, the air/sea buoyancy flux is a function of the sea-surface temperature, and therefore cannot be considered independent of the mean and eddy flow fields. Likewise in course-resolution models, the air/sea buoyancy flux, and hence subduction rates, and likely to depend implicitly on arbitrarily prescribed eddy transfer coefficients.

c. Parameterization of the eddy subduction. In a course resolution ocean model, one needs to parameterize the eddy subduction. The Gent and McWilliams (1990) scheme is a natural choice since it explicitly parameterizes the bolus velocity—the vehicle for the eddy subduction. Indeed the relation between the net subduction rate and surface buoyancy forcing, Eq. (16), perhaps represents an ideal surface boundary condition for Gent and McWilliams, since it relates the bolus velocity at the top of an adiabatic thermocline (where Gent and McWilliams is valid) to the buoyancy forcing of the surface mixed layer (within which Gent and McWilliams breaks down).

d. Southern Ocean uptake of anthropogenic carbon. Finally, ocean general circulation models have recently been used to infer the oceanic uptake of anthropogenic carbon (Maier-Reimer and Hasselmann, 1987; Sarmiento and Orr, 1992). Since air/sea tracer fluxes derived from numerical models depend on the subduction rate, which in turn depends on the air/sea buoyancy flux, the uncertainty associated with model-derived tracer fluxes can be no smaller than the corresponding uncertainty in the surface buoyancy fluxes. Within this context, discrepancies between model estimates of the uptake of anthropogenic carbon by the Southern Ocean and observed atmospheric carbon transports (Tans *et al.*, 1990) do not seem significant.

Acknowledgments. My thanks to Peter Gent, Amit Tandon, Elina Tragou, and two anonymous referees for suggesting improvements to the text. In particular, I wish to thank Ric Williams for many useful discussions and detailed comments on a preliminary draft. Various conversations with Mick Follows, Mei-Man Lee, John Marshall, Trevor McDougall, Malcolm Roberts, Kevin Speer, and Martin Visbeck are also appreciated. Travel grants were provided by The Royal Society and The University of Reading Research Board.

APPENDIX

The two-dimensional ocean model

Here a brief summary is given of the two-dimensional ocean model and its method of solution.

a. Southern Ocean. The model consists of a zonally-symmetric channel of dimensions 20 000 km × 2 000 km × 4 km. The channel is closed to the south ($y = 0$) by Antarctica,

but is open to the north ($y = y_0$); the sea surface is at $z = 0$ and the sea floor is at $z = -H$. The model incorporates a vertically-homogeneous mixed layer which overlies an adiabatic thermocline; the mixed layer depth, h, varies linearly with latitude except for a sharp increase adjacent to the southern boundary. The model is forced through a prescribed surface wind-stress, τ_s, a surface buoyancy flux, $\mathscr{B}_{in}$, and is dissipated through a prescribed zonal pressure gradient, $\Delta p/L$, where L is the length of the channel. Reynolds stresses and nonlinear accelerations are not considered.

The large-scale momentum equation can be written

$$-f\bar{v} + \frac{\Lambda \Delta p}{\rho_0 L} = \frac{1}{\rho_0}\frac{\partial \tau}{\partial z}. \tag{A1}$$

Here $\tau = \tau_s$ at the sea surface and decays to zero within a thin surface Ekman layer of thickness 30 m; $\Lambda = 0$ within the latitude and depth range of a prescribed Drake Passage where there is no zonal pressure gradient, and $\Lambda = 1$ elsewhere; the pressure gradient, Δp, varies with latitude such that the vertical integral of the zonal pressure gradient exactly balances the surface wind stress, that is

$$\frac{\Delta p}{L}\int_{-H}^{0} \Lambda dz = \tau_s.$$

Other parameters are:

$$\tau_s = \tau_0 \sin\left(\frac{\pi y}{y_0}\right)$$

where $\tau_0 = 0.1\ \mathrm{N\ m^{-2}}$, $f = -10^{-4}\ \mathrm{s^{-1}}$, and $\rho_0 = 10^3\ \mathrm{kg\ m^{-3}}$. The momentum equation (A1), and the continuity equation

$$\frac{\partial \bar{v}}{\partial y} + \frac{\partial \bar{w}}{\partial z} = 0,$$

completely determine the Eulerian-mean meridional circulation. The solution is

$$\bar{v} = -\frac{\partial \psi}{\partial z}, \qquad \bar{w} = \frac{\partial \psi}{\partial y},$$

where

$$\psi = \frac{1}{\rho_0 f}\left\{\tau - \frac{\Delta p}{L}\int_{-H}^{z} \Lambda dz\right\}. \tag{A2}$$

To solve for the eddy-induced circulation, we need to consider the thermodynamics. Within the adiabatic thermocline, the continuity equation is written most conveniently in isopycnic coordinates,

$$\left.\frac{\partial}{\partial y}\right|_{\rho}\left\{(\bar{v} + v^*)\frac{\partial \bar{z}}{\partial \rho}\right\} = 0. \tag{A3}$$

The bolus velocity is parameterized following Gent and McWilliams (1990),

$$v^* \frac{\partial \bar{z}}{\partial \rho} = -\kappa \left.\frac{\partial}{\partial y}\right|_\rho \frac{\partial \bar{z}}{\partial \rho}, \tag{A4}$$

where $\kappa = 500\ \mathrm{m^2\ s^{-1}}$ (chosen to give plausible isopycnal slopes across the ACC). Integrating (A3) with respect to both density (from the sea floor) and latitude gives

$$-\int_{-H}^{z(\rho)} (\bar{v} + v^*)\, dz = \psi(y, \rho) + \kappa \frac{\partial}{\partial y} \bar{z}(y, \rho) = C(\rho), \tag{A5}$$

The integration constants, $C(\rho)$, are determined by noting,

$$C(\rho_m) = -\int_{-H}^{-h} (\bar{v} + v^*)\, dz = -\int_0^y \overline{S}^{WM}\, dy,$$

and invoking the subduction formula (16) to give,

$$C(\rho_m) = -\frac{\mathscr{B}_{\mathrm{in}}}{g \partial \overline{\rho_m} / \partial y}. \tag{A6}$$

(The contribution of $\mathscr{B}_{\mathrm{eddy}}$ is negligible due to the large meridional extent of the domain and the uniform surface density gradient.) Eqs (A5) and (A6) are solved numerically for $\bar{z}(y, \rho)$, from which the bolus and transport circulations follow.

b. Convective chimney. The formulation and solution of the convective chimney in many respects mirrors the previous example, so only brief details are given. A cylindrically-symmetric domain of radius 200 km is considered in which a vertically-homogeneous mixed-layer overlies an adiabatic thermocline. The model is forced only by a prescribed surface buoyancy flux. As in the previous example, the Eulerian-mean circulation can be deduced directly from the momentum and continuity equations which, in the absence of wind forcing and Reynolds stresses, reduce very simply to

$$\bar{v} = \bar{w} = 0. \tag{A7}$$

Here v and w are the radial and vertical velocity components.

To determine the bolus circulation, we must again consider the thermodynamics. In cylindrical coordinates, the continuity equation becomes,

$$\left.\frac{\partial}{\partial r}\right|_\rho \left\{ r v^* \frac{\partial \bar{z}}{\partial \rho} \right\} = 0. \tag{A8}$$

The bolus velocity is again parameterized using Gent and McWilliams (1990),

$$v^* \frac{\partial \bar{z}}{\partial \rho} = -\kappa \left.\frac{\partial}{\partial r}\right|_\rho \frac{\partial \bar{z}}{\partial \rho}. \tag{A9}$$

For consistency, the same transfer coefficient ($\kappa = 500\ \mathrm{m^2\ s^{-1}}$) is used as in the Southern Ocean solutions, although this is perhaps on the upper end for a typical chimney. Applying

the same methodology as above gives,

$$r\kappa \frac{\partial}{\partial r} \bar{z}(r, \rho) = C(\rho), \tag{A10}$$

where

$$C(\rho_m) = -r \frac{(\mathscr{B}_{\text{in}} + \mathscr{B}_{\text{eddy}})}{g \partial \overline{\rho_m} / \partial r}. \tag{A11}$$

Here, the diapycnal mixing within the mixed layer is $O(1)$ and is parameterized as a simple diffusion,

$$\mathscr{B}_{\text{eddy}} = \gamma \frac{g}{r} \frac{\partial}{\partial r} \left\{ rh \frac{\partial \rho_m}{\partial r} \right\}. \tag{A12}$$

A smaller eddy transfer coefficient, $\gamma = 100\ \text{m}^2\ \text{s}^{-1}$, is chosen, primarily to prevent the convective chimney from being diffused away although one can also argue for the smaller coefficient on the grounds that air/sea fluxes damp eddy buoyancy transfer within the surface mixed layer (Treguier *et al.,* 1997). Solutions are obtained by prescribing $\mathscr{B}_{\text{in}}$ and $\mathscr{B}_{\text{eddy}}$ as boundary conditions, along with the vertical density profile at the outer boundary.

REFERENCES

Andrews, D. G. and M. E. McIntyre. 1976. Planetary waves in horizontal and vertical shear: The generalized Eliassen-Palon relation and the zonal mean acceleration. J. Atmos. Sci., *33,* 2031–2048.

—— 1978. An exact theory of nonlinear waves on a Lagrangian-mean flow. J. Fluid Mech., *89,* 604–646.

Cushman-Roisin, B. 1987. Subduction. Dynamics of the oceanic surface mixed layer, P. Muller and D. Henderson, ed. Hawaii Institute of Geophysical Special Publications, 181–196.

Danabasoglu, G. and J. C. McWilliams. 1995. Sensitivity of the global ocean circulation to parameterization of mesoscale tracer transports. J. Climate, *8,* 2967–2987.

Döös, K. and D. J. Webb. 1994. The Deacon Cell and the other meridional cells of the Southern Ocean. J. Phys. Oceanogr., *24,* 429–442.

Follows, M. J. and J. C. Marshall. 1994. Eddy driven exchange at ocean fronts. Ocean Model., *102,* 5–9.

Garrett, C., K. Speer and E. Tragou. 1995. The relationship between water mass formation and the surface buoyancy flux, with application to Phillip's Red Sea model. J. Phys. Oceanogr., *25,* 1696–1705.

Gent, P. R. and J. C. McWilliams. 1990. Isopycnal mixing in ocean circulation models. J. Phys. Oceanogr., *20,* 150–155.

Gent, P. R., J. Willebrand, T. J. McDougall and J. C. McWilliams. 1995. Parameterizing eddy-induced tracer transports in ocean circulation models. J. Phys. Oceanogr., *25,* 463–474.

Huang, R. X. and B. Qiu. 1994. Three-dimensional structure of the wind-driven circulation in the subtropical gyre of the North Pacific. J. Phys. Oceanogr., *24,* 1608–1622.

Lee, M.-M., D. Marshall and R. Williams. 1997. On the eddy transfer of tracers: diffusive or advective? J. Mar. Res., *55,* (in press).

Maier-Reimer, E. and K. Hasselmann. 1987. Transport and storage of CO_2 in the ocean—an inorganic ocean-circulation cycle model. Clim. Dyn., *2,* 63–90.

Marshall, J. C. and A. J. G. Nurser. 1992. Fluid dynamics of oceanic thermocline ventilation. J. Phys. Oceanogr., *22,* 583–595.

Marshall, J. C., A. J. G. Nurser and R. G. Williams. 1993. Inferring the subduction rate and period over the North Atlantic. J. Phys. Oceanogr., *23,* 1315–1329.

McDougall, T. J. 1991. Parameterizing mixing in inverse models, *in* Dynamics of Oceanic Internal Gravity Waves, P. Muller and D. Henderson, eds., Proc. Sixth 'Aha Huliko'a Hawaiian Winter Workshop, University of Hawaii at Manoa, 355–386.

McDougall, T. J. and P. C. McIntosh. 1996. The temporal-residual-mean velocity: I. Derivation and the scalar conservation relations. J. Phys. Oceanogr., *26,* 2653–2665.

McIntosh, P. C. and T. J. McDougall. 1996. Isopycnal averaging and the residual mean circulation. J. Phys. Oceanogr., *26,* 1655–1660.

Nurser, A. J. G., R. Marsh and R. G. Williams. 1997. Diagnosing water mass formation from air-sea fluxes and surface mixing. J. Phys. Oceanogr., (submitted).

Nurser, A. J. G. and J. C. Marshall. 1991. On the relationship between subduction rates and diabatic forcing of the mixed layer. J. Phys. Oceanogr., *21,* 1793–1802.

Plumb, R. A. and J. D. Mahlman. 1987. The zonally averaged transport characteristics of the GFDL General Circulation Model. J. Atmos. Sci., *44,* 298–327.

Pollard, R. T. and L. A. Regier. 1992. Vorticity and vertical circulation at an ocean front. J. Phys. Oceanogr., *22,* 609–625.

Rhines, P. B. 1982. Basic dynamics of the large-scale geostrophic circulation. Summer Study Program in Geophysical Fluid Dynamics, Woods Hole Oceanographic Institution, 1–47.

Sarmiento, J. L. and J. C. Orr. 1992. A perturbation simulation of CO_2 uptake in an ocean general circulation model. J. Geophys. Res., *97,* 3621–3645.

Send, U. and J. C. Marshall. 1995. Integral effects of deep convection. J. Phys. Oceanogr., *25,* 855–872.

Spall, M. A. 1995. Frontogenesis, subduction and cross-front exchange at upper-ocean fronts. J. Geophys. Res., *100,* 2543–2557.

Speer, K. and E. Tziperman. 1992. Rates of water mass formation in the North Atlantic Ocean. J. Phys. Oceanogr., *22,* 93–104.

Tandon, A. and C. Garrett. 1996. On a recent parameterization of mesoscale eddies. J. Phys. Oceanogr., *26,* 406–411.

Tans, P. P., I. Y. Fung and T. Takahashi. 1990. Observational constraints on the global atmospheric CO_2 budget. Science, *247,* 1431–1438.

Treguier, A. M., I. M. Held and V. D. Larichev. 1997. On the parameterization of quasi-geostrophic eddies in primitive equation ocean models. J. Phys. Oceanogr., (in press).

Tsuchiya, M., L. D. Talley and M. S. McCartney. 1994. Water-mass distributions in the western South Atlantic; a section from South Georgia Island (54S) northward across the equator. J. Mar. Res., *52,* 55–81.

Tung, K. K. 1987. A coupled model of zonally averaged dynamics, radiation and chemistry, *in* Transport Processes in the Middle Atmosphere, G. Visconti and R. Garcia, eds., 183–198.

Visbeck, M., J. C. Marshall and H. Jones. 1996. Dynamics of isolated convective regions in the ocean. J. Phys. Oceanogr., *26,* 1721–1734.

Walin, G. 1982. On the relation between sea-surface heat flow and thermal circulation in the ocean. Tellus, *34,* 187–195.

Received *7 May, 1996;* revision: *5 November, 1996.*